https://doi.org/10.5194/egusphere-2023-785
Preprint. Discussion started: 15 May 2023

Data treatment and corrections for estimating H_2O and CO_2 isotope fluxes from high-frequency observations

Robbert P.J. Moonen[1], Getachew A. Adnew[1], Oscar K. Hartogensis[2], Jordi Vilà-Guerau de Arellano[2], David J. Bonell Fontas[1], and Thomas Röckmann[1]

[1]Institute for Marine and Atmospheric Research, Utrecht University,
[2]Meteorology and Air Quality Group, Wageningen University,

Correspondence: Robbert Moonen (r.p.j.moonen@uu.nl)

Abstract. Current understanding of land-atmosphere exchange fluxes is limited by the fact that available observational techniques mainly quantify net fluxes, which are the sum of generally larger, bi-directional fluxes that partially cancel out. As a consequence, validation of gas exchange fluxes applied in models is challenging due to the lack of ecosystem-scale exchange flux measurements partitioned into soil, plant, and atmospheric components. One promising experimental method to partition measured turbulent fluxes uses the exchange-process-dependent isotopic fractionation of molecules like CO_2 and H_2O. When applying this method at a field scale, an isotope flux (δ-flux) needs to be measured. Here, we present and discuss observations made during the LIAISE 2021 field campaign using an Eddy Covariance (EC) system coupled to two laser spectrometers for high frequency measurement of the isotopic composition of H_2O and CO_2. This campaign took place in the summer of 2021 in the irrigated Ebro River basin near Mollerussa, Spain, embedded in a semi-arid region.

We present a systematic procedure to scrutinise and analyse the measured values of central δ-flux variable. Our experimental data indicated a larger relative signal loss in the δ-fluxes of H_2O compared to the net ecosystem flux of H_2O, while this was not true for CO_2. Furthermore, we find that mole fractions and isotope ratios measured with the same instrument can be offset in time by more than a minute for the H_2O isotopologues. We discuss how such artifacts can be detected and how they impact flux partitioning. We argue that these effects are likely due to condensation of water on a cellulose filter in our inlet system. Furthermore, we show that these artifacts can be resolved using physically sound corrections for inlet delays and high frequency loss. After such corrections and verification's are made, isotopic ecosystem scale flux partitioning can be used reliably to validate conceptual land-atmosphere exchange models.

1 Introduction

Net ecosystem flux measurements of ET and NEE are used at many sites worldwide to study exchange of water and CO_2between the biosphere and atmosphere. These net fluxes are the sum of partial flux components which are often larger than the net flux and compensate each other. Each of these gross flux components has unique sources and dependencies on environmental variables. The Gross Primary Production (GPP) is dependent on variables like Photosynthetic Active Radiation (PAR) and the Vapour Pressure Deficit (VPD) (van Diepen et al., 2022). On the other hand, ecosystem Respiration (R_{eco}), has strong links

https://doi.org/10.5194/egusphere-2023-785
Preprint. Discussion started: 15 May 2023

to soil and leaf temperatures and water contents. Importantly, such environmental dependencies are used in atmospheric models to predict the evolution of gross and net exchange fluxes in a future changing climate. Thus, to properly validate model parameterization, we need ecosystem scale flux measurements of the gross components.

One promising method that allows for flux partitioning uses the stable isotopic composition of the exchanged molecules. A trace gas has multiple stable isotopologues, or molecules with a given isotopic configuration, which undergo exchange processes at slightly different rates. As the various exchange fluxes are caused by different physio-chemical processes, the isotopic fractionation differs between them. The combined effect of all fractionation processes can be measured on atmospheric molecules and used to partition net exchange fluxes.

On the global scale, isotopic partitioning has been used to separate annual NEE into GPP and R_{eco}, using the global mean isotopic signature of $\delta^{18}O$ in CO_2 (Prentice et al., 2001). On smaller spatiotemporal scales (hourly, local), the same principal can be used to split NEE into GPP and R_{eco}, and Evapotranspiration (ET) into Evaporation (E) and Transpiration (T) (Lee et al., 2009; Vilà-Guerau de Arellano et al., 2020). Doing so allows us to better understand, and consequently model, the drivers of each flux component, including non-linear short term (diurnal, sub-diurnal) effects (Vilà-Guerau de Arellano et al., 2023). When using isotopic partitioning on small spatiotemporal scales, a framework like the one described by Oikawa et al. (2017) can be used. They clarify that the key variable that needs to be measured is a turbulent iso-flux.

Two decades ago, isotopic compositions measured with laser spectrometers got precise enough to allow for gradient based flux methods (Griffis et al., 2004, 2007). Some years later, it was shown that high sample throughput and precision could be achieved to perform direct flux measurements by combining stable isotope measurements with Eddy Covariance (EC) (Sturm et al., 2012; Griffis, 2013). Since then, measurement of iso-fluxes have been made with instruments that measure isotopic compositions at high temporal resolution (faster than 1Hz). Various research group have contributed to advancing this combined technique (Wehr and Saleska, 2015; Oikawa et al., 2017; Wahl et al.; Sturm et al., 2012; Griffis, 2013). Still, there is much to be learned about δ-fluxes, the challenges in measuring them and how to correct sub-optimal data (Oikawa et al., 2017). In this manuscript, we describe the methods and measurement setup we used for making δ-flux measurements of both H_2O and CO_2 in the field. We present data from the LIAISE field campaign which took place in July 2021 in the Ebro river basin in the northeast of Spain. In this study we focus on the challenges associated with the setup, and evaluation of the experimental isotope (flux) data. We present measurement artifacts, the most likely causes, and correction methods we applied. Finally, we share our outlook on flux partitioning and highlight the potential for minute scale δ-flux measurements.

2 Theory

H_2O and CO_2 molecules in the natural environment consist of all possible combinations of the light and heavy hydrogen, oxygen and carbon isotopes. Since the abundance of the heavy isotopes is very low (D/H = $1.6e^{-4}$, $^{17}O/^{16}O$ = $3.8e^{-4}$, $^{18}O/^{16}O$ = $2.0e^{-3}$, $^{13}C/^{12}C$ = $1.1e^{-2}$), heavy isotopologues are much less abundant than the light isotopologues ($H_2^{16}O$ and $^{12}C^{16}O_2$), and are therefore much more difficult to measure at high precision. An additional difficulty is that the natural variations in isotopic compositions, for example due to fractionation during gas exchange in plants leaves or soil, are small. For that reason,

https://doi.org/10.5194/egusphere-2023-785
Preprint. Discussion started: 15 May 2023

isotope ratios are reported in δ notation, that is, as a deviation of the heavy-to-light isotope ratio compared to that ratio in a reference sample (Mook and Geyh, 2000).

$$\delta^h X = \frac{{}^h R_{spl}}{{}^h R_{ref}} - 1 = \frac{\left[\frac{{}^h X}{{}^l X}\right]_{spl}}{\left[\frac{{}^h X}{{}^l X}\right]_{ref}} - 1 \quad (1)$$

Here, X represents an element, h represents a heavy isotope of that atom, l the abundant (i.e. light) isotope, "$_{spl}$" the measured sample, and "$_{ref}$" the reference. For hydrogen and oxygen atoms, the Vienna Standard Mean Ocean Water (VSMOW) is the common reference (D/H = 1.5576e^{-4}, ^{18}O/^{16}O = 2.00520e^{-3}), while for carbon this is Vienna Pee Dee Belemnite (VPDB, ^{13}C/^{12}C=1.1180e^{-2}) (IAEA, 2017; Craig, 1957).

2.1 Isotope effects associated with land-atmosphere exchange

Different processes that facilitate exchange of H_2O and CO_2 between the earth's surface, plants, and the atmosphere, are associated with isotope fractionation. One example is evaporation. As liquid water evaporates, light isotopologues evaporate preferentially compared to heavy isotopologues. This is due to the comparatively higher saturation vapour pressure of light H_2O compared to heavy H_2O (Horita and Wesolowski, 1994). Another example is the diffusion of gases through small openings such as stomata, where the light isotopologues enter and leave the stomata at a slightly faster rate than the heavy isotopologues. This is caused by the higher velocity of lighter isotopologues (Mook and Geyh, 2000). Also, photosynthesis itself causes fractionation as ^{12}C is preferentially taken up by RuBisCO, resulting in a slight enrichment in the δ^{13}C of CO_2 remaining in the atmosphere (Farquhar et al., 1989; Adnew et al., 2020).

The preferential uptake or emission of light or heavy isotopologues at the land-atmosphere interface, combined with turbulent transport in the boundary layer, leads to vertical gradients of the different isotopologues, and thus the δ-values, in the boundary layer. These gradients are conceptually visualized in Figure 1. For H_2O, plant transpiration is generally enriched in ^{18}O compared to the atmospheric reservoir (Yakir et al., 2006). This leads to negative atmospheric gradients ($\frac{\Delta\delta^{18}O}{\Delta z}$) of δ^{18}O which will result in a positive (upward) δ-flux (Sect. 2.2). For CO_2, the main driver of the gradients is photosynthetic uptake. CO_2 near the surface gets enriched in ^{13}C-CO_2, again leading to upward transport of δ^{13}C, which is in this case opposite to the flux of CO_2itself.

2.2 δ-flux definitions

Turbulent vertical mixing of air in the boundary layer results in a reduction of the concentration and isotope gradients that are illustrated in Fig 1. For the isotopic compositions, expressed as δ-values, this results in a δ-flux.

$$F_\delta = \overline{w'\,\delta'} \quad (2)$$

https://doi.org/10.5194/egusphere-2023-785
Preprint. Discussion started: 15 May 2023

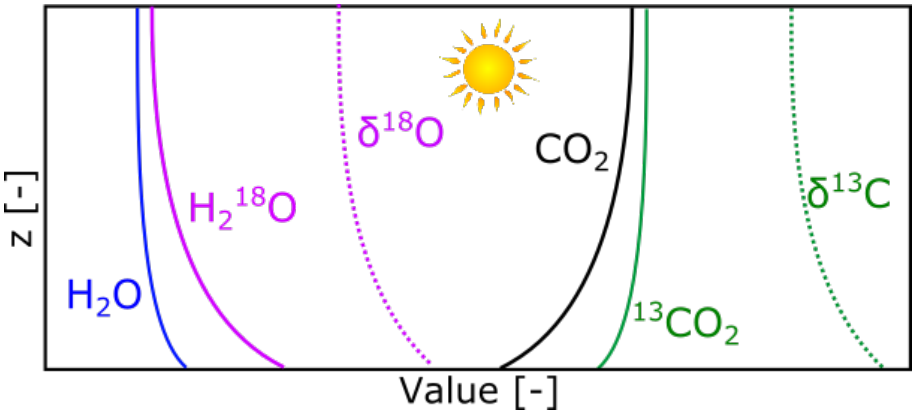

Figure 1. Conceptual visualization of the gradients of mole fractions and δ-values in the atmospheric surface layer (ASL) during midday ($z/L_{ob} < 0$) over a vegetated area.

Here, F_δ is the δ-flux in $‰\,\mathrm{m\,s^{-1}}$, w' represents the perturbations in the vertical wind speed in $\mathrm{m\,s^{-1}}$, and δ' the perturbations in the δ-values of the molecule in question. Lee et al. (2012) and peers, refer to the δ-flux variable as an iso-forcing since it links the isotopic composition of the flux source to a pertubation in the atmospheric isotopic composition. From an experimental perspective, naming it a δ-flux best expresses that we are referring to a flux of measured δ-values. Note that, for isotopic flux partitioning, an other type of flux with units $\frac{‰\,\mathrm{mol}}{\mathrm{m^2\,s}}$ is required, which we refer to as iso-flux. The δ-flux is directly linked to this iso-flux, and is the key, hard-to-measure, part of it. Conceptually, Eq. (2) indicates that the magnitude of the δ-flux is proportional to the gradient in the δ-values (visualized in Fig. 1), which determines the magnitude of the anomalies δ', and the vertical mixing intensity expressed by w'.

Next to the δ-flux, we also derive the isotopic composition of the flux itself ($\delta^h X_F$, Eq. 3), which can be interpreted as the isotopic composition at the exchange interface (Griffis et al., 2004; Lee et al., 2012). Together with the atmospheric isotopic composition, this variable allows us to describe the strength and sign of the isotopic gradient (in $‰\,\mathrm{z^{-1}}$) in the atmospheric surface layer. See Fig. 1 for an example of such a gradient. The isotopic composition of the flux can be derived using either the volume flux ratios of the major and minor isotopologues or by combining the δ-flux, $\delta^h X_{atm}$, the net exchange flux, and the atmospheric concentration of the molecule.

$$\delta^h X_F = \frac{{}^h R_F}{{}^h R_{ref}} - 1 = \delta^h X_{atm} + F_\delta \frac{C_x}{F_x} \tag{3}$$

$${}^h R_F = \frac{\overline{w'\,q'_{h_x}}}{\overline{w'\,q'_{l_x}}} * \frac{1}{n} \tag{4}$$

Here, $\delta^h X_F$ is the isotopic composition of the flux, ${}^h R_F$ is a ratio of isotopologue fluxes, q'_{h_x} represents the deviations in the mass fraction of an isotopologue with respect to the 30 minute mean. $\delta^h X_{atm}$ is the atmospheric isotopic composition

https://doi.org/10.5194/egusphere-2023-785
Preprint. Discussion started: 15 May 2023

of the compound, C_x is the total concentration of the molecule in $\mathrm{mol\,m^{-3}}$, F_x is the flux of the molecule in $\mathrm{mol\,m^{-2}\,s^{-1}}$, and n indicates the number of places within the molecule where the rare isotope can be substituted. When only one process (e.g. photosynthesis) with a given fractionation influences the atmospheric composition, $\delta^h X_F$ - $\delta^h X_{atm}$ should be equal to the magnitude of that fractionation (Fig. 1). In more complex environments, $\delta^h X_F$ - $\delta^h X_{atm}$ is still good indicator of which process is dominant, given that the respective fractionation effects are known. Together, F_δ and $\delta^h X_F$ are variables that complement the more common $\delta^h X_{atm}$ and net gas exchange measurements by linking them to the physio-chemical processes in the flux footprint.

3 LIAISE field campaign

3.1 Site description

We performed δ-flux measurements during the LIAISE (Land surface Interactions with the Atmosphere over the Iberian Semi-arid Environment) field campaign in the summer of 2021 (Boone et al., 2021). This campaign took place in the irrigated Ebro basin near Mollerussa, Spain. The focus of the effort was to investigate the effects of large scale irrigation on the atmospheric boundary layer and large scale circulation (Mangan et al., 2023). Iso-flux measurements were made in the middle of a field with flood irrigated alfalfa (C3), a fast growing crop with large ET that was not radiation or water limited. The alfalfa grew from 50 to 65 cm above ground level during the measurement period described in this manuscript (25-30 July) and covered the entire field during that period. Importantly, the combination of large ET and GPP caused significant isotopic fractionation effects and related iso-fluxes with diurnal cycles to emerge. Flood irrigation took place once during the campaign, two days before our isotope measurement period started. During the measurement period one precipitation event occurred ($26^t h$). Otherwise, measurement days showed a comparable diurnal weather cycle with largely clear sky conditions and some cirrus, $32^\circ\mathrm{C}$ mean peak temperatures, and 650 $\mathrm{Wm^{-2}}$ mean peak net radiation. Wind speeds at 2.45 m were below 2.5 $\mathrm{ms^{-1}}$ for 90% of the time, while the wind direction alternated between easterly and south westerly due to a sea breeze circulation. The presence of comprehensive measurements of auxiliary variables (like soil moisture contents, stomatal aperture, etc.) will allow us to investigate the iso-fluxes and their main drivers environmental in later work (Mangan et al., 2023; Boone et al., 2021).

3.2 Setup

The Iso-flux setup consisted of an Eddy Covariance (EC) station with the addition of two laser spectrometers. The EC station was an IRGASON EC-100 (Campbell Scientific, Logan, USA), which combines a Sonic Anemometer with an Open Path Gas Analyser (OPGA; Fig. 2). It was installed on a tripod at 2.45 m above ground level and faced South (180°). 20 cm below the anemometer's center an inlet line continuously sampled atmospheric air for analysis in the laser spectrometers. The tubing and instruments downstream were kept free from dust and insects using a Whatmann cellulose thimble inlet filter. To prevent the bulky inst enclosures from impacting the turbulence measurements, they were placed away from the EC mast and connected via a 9 m inlet line (3/8" OD tubing). This inlet was kept to a reasonably short length to prevent mixing of air samples in the

https://doi.org/10.5194/egusphere-2023-785
Preprint. Discussion started: 15 May 2023

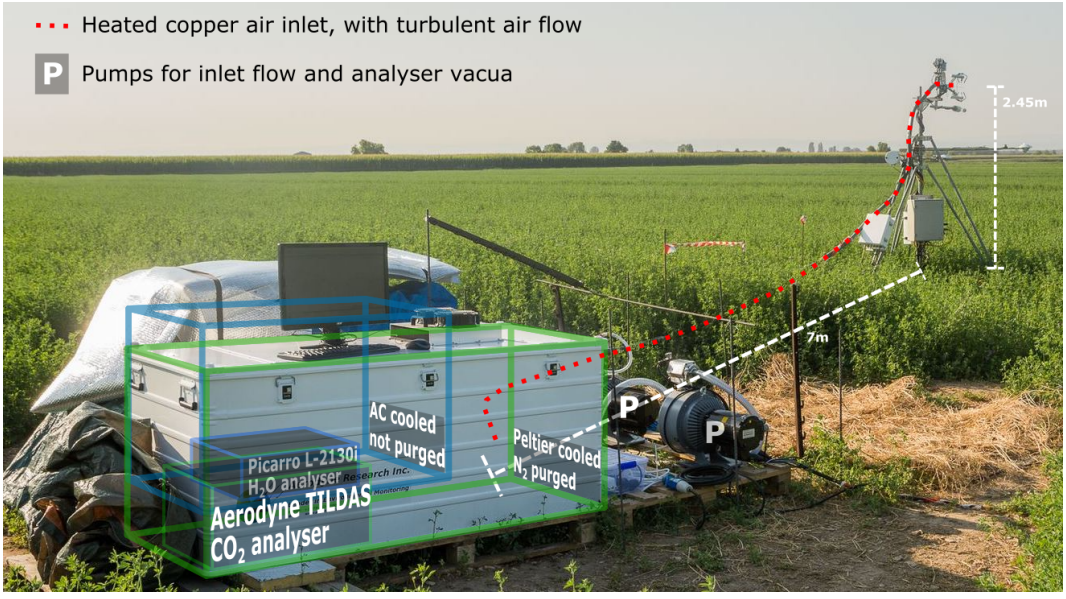

Figure 2. Picture of the iso-flux measurement setup (taken by Wouter Mol, wbmol@wur.nl), overlayed with a schematic overview of the measurement setup. The instrument and enclosure outlined in green indicate the CO_2 isotopologue setup. The instrument and enclosure outlined in blue indicate the H_2O isotopologue setup, which is behind the CO_2 enclosure in the picture.

inlet. Turbulent flow inlet conditions (Re > 3000) were generated using an air flow rate of 30 $\mathrm{l\,min^{-1}}$. 20 $\mathrm{l\,min^{-1}}$ of that flow was generated with a dedicated inlet scroll pump. The rest was generated from the suction of the laser spectrometers. To reduce isotopic exchange between the air and the wall of the inlet tube, the copper inlet line and heated to a 50°C setpoint using a heating wire and tube isolation.

Downstream of the main inlet, 0.9 $\mathrm{l\,min^{-1}}$ of air was directed to a Picarro L2130-i laser spectrometer (Picarro, Santa Clara, USA) m measuring H_2O isotopologues (H_2O, DHO, $H_2^{18}O$) and modified to run at higher sample flow-rates. Another 9 $\mathrm{l\,min^{-1}}$ was directed to an Aerodyne TILDAS-CS laser spectrometer (Aerodyne Research, Billerica, USA) measuring CO_2 isotopologues (CO_2, $^{13}CO_2$, $CO^{18}O$). These instruments have measurement frequencies of 4 Hz and 10 Hz respectively, which in principle allows for eddies of the smallest turbulent scales (cm) to be distinguished (Moene and Van Dam, 2014). Both instruments were installed in weatherproof, temperature controlled enclosures which were placed on pallets to protect them from (flood irrigation) water and dirt.

For the TILDAS-CS, we used a field enclosure manufactured by Aerodyne Inc., which we purged with N_2 to prevent CO_2 absorption in the instruments optics (Fig. 2). Additionally, the dry N_2 prevents water from condensing on the Peltier thermoelectric cooler used in the setup. The temperature setpoint in the enclosure was 35°C, matching the setpoint of the liquid coolant stabilizing the analysers internal temperature. Still, we observed diurnal variations in the power of the analyser's liquid chiller unit (OASIS), which affected the observed isotopic composition of atmospheric CO_2 (Sect. 5.2).

https://doi.org/10.5194/egusphere-2023-785
Preprint. Discussion started: 15 May 2023

The Picarro H_2O isotopologue monitor was placed in a custom built, insulated enclosure which was temperature controlled and dried using a compact AC unit set to 28°C (Fig. 2). Purging the enclosure with dry air was not required as the optical path in the instrument is short which minimizes out-of-cell light absorption (Picarro, 2021). An AC unit increases the risk of water condensation compared to a Peltier element due to the on-off nature of control. While the analyser's setpoint of 80°C for the sample cell prevents water condensation internally, the inlet tubing is vulnerable to cold pulses. To reduce the external heating from solar radiation and thus the required cooling power, we installed reflective sun-shielding at 15 cm above the lid of the enclosure, allowing for ventilation.

The vacuum pumps providing the required low pressure to the analysers were placed next to the enclosures on another pallet together with the inlet pump, 4G modem, and inlet temperature controller. A roof of wetted hay provided shielding from the sun and evaporative cooling of the air passing over the pumps. During rain events, a tarp was installed instead. The enclosures and peripherals were located perpendicular to the main wind directions with respect to the EC system to prevent footprint disruptions.

4 Data treatment

4.1 Calibrations

Laser spectrometers require regular calibrations for accurate measurements of the concentration or isotopic composition of the target species. Griffith (2018) gives an excellent overview of suitable calibration procedures stating that conceptually, two effects need to be addressed by calibration: 1) the dependence of the δ-values on mole fractions and 2) the span calibration, or, the calibration of the isotopic against a reference standard. δ-flux measurements do not require high accuracy but mainly need high precision, because detrended fluctuations in δ-values are used to derive the 30 minute δ-flux (Eq. 2). Longer timescale instrument drift and related uncertainty in the absolute isotopic composition are thus removed from the signal (Griffis et al., 2010; Van Kesteren et al., 2013). For this reason, frequent span calibrations were not our priority and we determined the span calibrations and mole fraction dependency of the δ-values in the lab before and after the campaign. However, mole fraction calibrations are key for δ-flux measurements because the variations in atmospheric isotopic compositions are naturally associated with variations in mole fraction, and thus a dependence of the isotopic composition on mole fraction represents a first order interference with the target signal.

The L2130-i was calibrated with a commercial Standards Delivery Module (SDM, Picarro, Santa Clara, USA). Two liquid standards that spanned the range of values measured on site were used. One was demineralized tap water from the Netherlands (52°N) and the other was melt water from ice-cores from Greenland (75°N). Both were linked to the VSMOW scale using reference standards from the IAEA (Tb. 1).

Differences in the span calibrations performed before and after the campaign were $\pm 0.4‰$ for $\delta^{18}O$ and $\pm 0.3‰$ for δD at atmospheric isotopic compositions. Drift during the measurement period was below $0.1‰$ for both species when assuming drift to behave linearly. Likely, the drift during field measurements was even smaller given that instrument rebooting and transportation cause more drift than continuous operation. The consistency in the mole fraction calibrations is indicated in

https://doi.org/10.5194/egusphere-2023-785
Preprint. Discussion started: 15 May 2023

Table 1. The isotopic compositions of the H_2O calibration standards and approximate atmospheric isotopic composition during the measurement period

	δ^{18}**O**	δ**D**
NL tap water	-6.98‰	-47.12‰
GL icecore	-30.80‰	-240.86‰
LIAISE atm	-12‰	-100‰

Fig. 3. Note that the mole fraction calibration curves reveal a cross dependency on the isotopic composition. The origin could not be precisely identified but we suspect that a small leak of ambient air during calibrations could cause this issue. In that case, the ratio of ambient to calibration vapour differed dependent on H_2O concentration, and thus affected the measured isotopic composition. To reduce the effect of this contamination on the coefficients of the calibration fit, we interpolated the coefficients linearly between the two standards to approximate the isotopic composition of the atmosphere. The resulting weighting between the coefficients of the two standards is described by (3 NL tap water + 1 GL ice core) / 4. We suggest that the similarity in the "Weighted Avg" calibration coefficients before and after the campaign in Fig. 3 is no coincidence, but a feature of an ambient air leak of variable magnitude. Note that some studies have found instrument related cross dependency of the isotopic composition on the mole fraction dependence (Weng et al., 2020).

The TILDAS-CS was calibrated using a GASMIX AIOLOS 2 (AlyTech, Juvisy-sur-Orge, France). For the span calibrations we used two standards with known isotopic compositions. Next to that, a 8000 $\mu mol\,mol^{-1}$ CO_2 canister was diluted with synthetic air (N_2, O_2, Ar) using a mixing scheme to derive the mole fraction dependence (Tb. 2). During the campaign we observed slow 5 ‰ variations in the δ-values with a diurnal cycle related to instrument housekeeping variables. Consequently, we have little confidence in the measured absolute atmospheric isotopic composition. However, as discussed before, we do not need long term accuracy but short term precision to derive the isotope fluxes. Important to note is that later experiments with similar housekeeping-related drift revealed that mole fraction dependencies remain unaffected (Appendix A1).

Table 2. The calibration coefficients of δ-values to CO_2 mole fractions in $\mu mol\,mol^{-1}$, as derived after the campaign.

Mole fraction dependence	δ^{18}**O**	δ^{13}**C**
Linear	-1.27e-2	-3.64e-2
Quadratic	1.80e-6	1.16e-5

https://doi.org/10.5194/egusphere-2023-785
Preprint. Discussion started: 15 May 2023

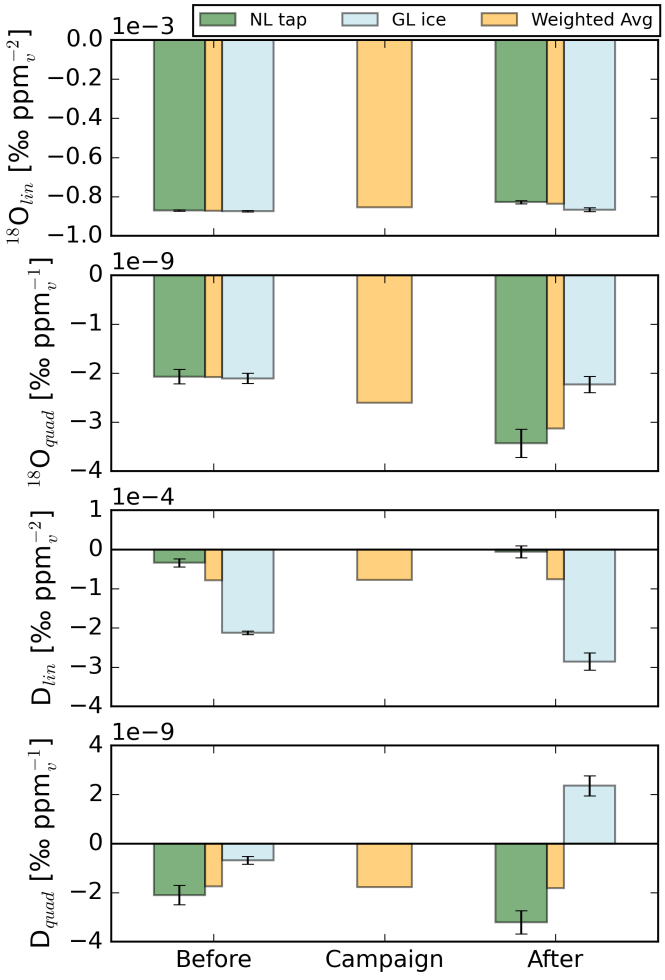

Figure 3. Calibration coefficients for solving the mole fraction dependence (δD_{mol} = D_{quad} * $H_2O^2_{ppm_v}$ + D_{lin} * $H_2O_{ppm_v}$), derived before and after the LIAISE campaign for the L2130-i H_2O isotopologue analyser. The yellow bars at the "Before" and "After" moments indicate the virtual calibration coefficients, i.e., what the coefficients would have been when the water standard would have had an isotopic composition similar to the atmospheric isotopic composition. As this minimized inlet contamination effects these coefficients are the ones we worked with. "Campaign" represents the value these virtual coefficients would have had during the measurement campaign in case of linear drift, and are the coefficients we used to correct our measurements with.

4.2 Time shift corrections

A practical issue when combining high frequency data from two separate instruments, in our case laser spectrometers and EC, are non-synchronous and drifting data logger clocks in addition to inlet time lag. In order to synchronize two high frequency time series of related atmospheric variables in post processing, we used a correlation coefficient (R^2) based alignment scheme

https://doi.org/10.5194/egusphere-2023-785
Preprint. Discussion started: 15 May 2023

that works as follows (similar to Fan et al. (1990)). After the two time series are coarsely aligned using known clock offsets, 10 minute sections were sliced from the longer time series. One of the sections is subsequently cropped by a minute on each side which makes it possible to shift it in time with respect to the other section within this (two) minute window. Here, the minimal time shift is the measurement interval of the highest frequency time series. For each of these unique time shifts a correlation coefficient (R^2) can be calculated between the time series. Note that for deriving R^2, the high frequency time series should be sub-sampled to the frequency of the low frequency time series. The maximum value of R^2 over the range of time shifts indicates the shift of optimal correlation and thus the most probable offset in the clocks. We sped up the time alignment by first deriving the R^2 for a subset of time shifts to find the approximate optimum. Subsequently, we filled in the missing R^2 values but only around the approximate optimum. Fig. 4 shows an example of the derived time drift between the H_2O signal of a laser spectrometer and an EC station over a day at two hour intervals. Note that the data logger clocks drifted near linearly in this example. By adjusting the time for each 10 minute section using the derived time shift we constructed one synchronised data set unaffected by data logger clock drift or inlet line related time lags.

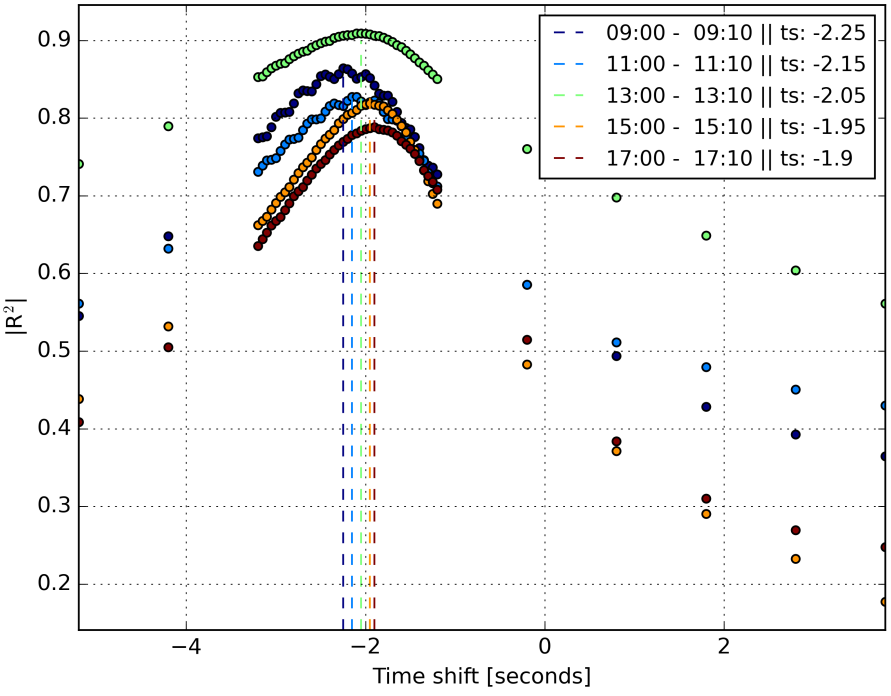

Figure 4. Example of the R^2-based time shifts algorithm in action. In this case the shift between the EC station and the Picarro L2130-i is determined using the H_2O mole fraction measurements of both instruments. The different colors each represent a 10 minute section of data on July 25^{th}, as indicated in the legend. Each dashed vertical line indicates the optimal time shift of the two 10 minute data sections. The derived time shift values are provided in the legend. A negative time shift indicates that the laser spectrometer is delayed compared to the EC system. Note that during this period the instrument clocks were drifting approximately linearly with respect to each other.

https://doi.org/10.5194/egusphere-2023-785
Preprint. Discussion started: 15 May 2023

4.3 Spectral corrections

Open path gas analysers are known to capture high frequency contributions to gas exchange fluxes better compared to closed path instruments. This is because the smallest spatiotemporal eddy scales are missed by closed path instruments due to inlet line signal attenuation and sample cell retention times (Spank and Bernhofer, 2008). The same is true for the closed path laser spectrometers we use for isotopologue measurements. In this section we detail how we corrected for the lost high frequency signal of both the mass fluxes and delta fluxes using the mole fraction signal from the EC system.

4.3.1 Mole fraction correction

To compare the mass fluxes derived using the EC and the isotopologue instruments, we used cospectra of the fluctuations in w and CO_2 or H_2O. Such spectra are based on a Fast Fourier Transform (FFT) of a 30 minute data interval and express the contribution to the covariance between two signals as a function of frequencies. In Fig. 5, cospectra of the vertical wind speed (w [$\mathrm{m\,s^{-1}}$]) with specific humidity and CO_2 (q [$\mathrm{kg\,kg^{-1}}$]) are shown.

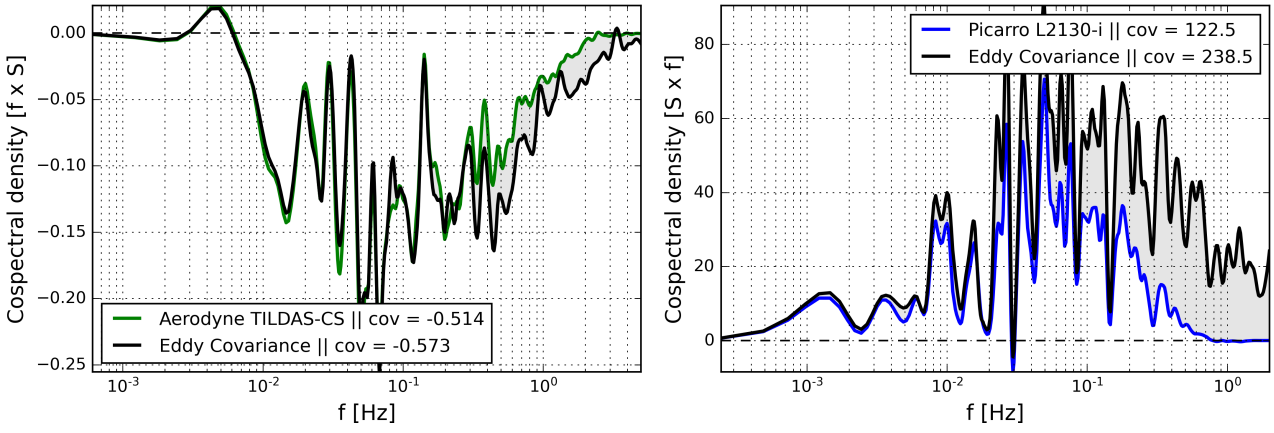

Figure 5. Comparison of the cospectra of w′ and q′ from both the closed path laser spectrometers and the OPGA of the Eddy Covariance station. The left panel represents the CO_2-w cospectra, and the right panel the H_2O-w cospectra. The spectra are based on a 30 minute data interval taken during the measurement period starting at 12:00 on July 25^{th} 2021.

It is apparent from Fig. 5b that a significant part of the total exchange flux, mostly at higher frequencies, was not captured by the Picarro L2130-i. The TILDAS-CS CO_2 isotopologue analyser suffered to a much smaller extend from such high frequency signal loss and captured cospectra similar to the ones derived using the OPGA. When iso-fluxes are measured with OPGA measurements no high frequency signal is lost, so correcting net flux spectra is not required. In case only closed path measurements are used, some correction is needed. One such correction is explained in Spank and Bernhofer (2008) and works by deriving a transfer function for the closed path instrument to correct for the reduced high frequency signal. However, the

https://doi.org/10.5194/egusphere-2023-785
Preprint. Discussion started: 15 May 2023

observed high frequency loss can also affect single isotopologue flux cospectra and δ-flux cospectra, and therefore needs to be taken into account in some way, optionally through using the signal loss in the net flux measurement.

4.3.2 δ-value correction

As suggested in the previous section, the fraction of the missed mole fraction signal is one way to estimate how much high frequency signal is likely lacking from isotopologue and δ-fluxes. This approach has been applied in several other studies (e.g. Wahl et al.; Oikawa et al. (2017); Wehr et al. (2013)), for example through the use of cumulative cospectra (Ogives) of the $w'q'$ between an OPGA and a laser spectrometer. By correcting the high frequency loss of each isotopologue for the loss in net flux, the δ-flux is implicitly increased by the same loss factor (see Eq. 3 & 4).

$$CF^{x}_{opga} = \frac{cov[w'q'_x]_{opga}}{cov[w'q'_x]_{cpga}} \equiv \frac{\int S^{w'q'}_{opga}(f)\, df}{\int S^{w'q'}_{cpga}(f)\, df}. \tag{5}$$

Here, CF^{x}_{opga} is the correction factor based on the flux measured using a closed path or open path analyser, and S represents the frequency dependent cospectral density (as plotted on the y-axis in e.g. Fig. 5).

Investigation of the cospectra of δ-fluxes and net exchange fluxes revealed that the shapes of both are related at all frequencies for our CO_2 isotope measurements (Appendix A3). Strikingly, this is not true for the H_2O isotope measurements. Fig. 6 indicates that the cospectra of $\delta^{18}O$ and H_2O with respect to w', e.g. the purple and the black lines, are similar only on timescales >100 s, while at faster timescales there are strong differences. The general trend, sign, and small features around 4x10^{-3} Hz and 8x10^{-}3 Hz match well. However, at shorter timescales, the $\delta^{18}O$ spectrum progressively diminishes to noise. In contrast, the net H_2O exchange spectrum remains positive with significant contributions to the total exchange flux in this high frequency region.

We propose that the reason for this missing δ-flux signal is a sub-optimal setup rather then a true land-atmosphere exchange phenomenon (Sect. 6). Given the overlap in spectral shapes at the low frequency side, we designed a spectral scaling approach for finding a δ-flux correction for the signal loss at the high frequency side. The key reasoning behind our approach is that the cospectral shape of a δ-flux should be identical to the shape of the total exchange flux. This implies that eddies of any size which transport isotopically modified H_2O or CO_2 have proportionally altered mixing ratios and δ-values. In other words, we assume that each exchange process with its unique fractionation effects contributes to the total δ-flux at all eddy sizes (Sect. 6).

To correct for this loss in signal we use the re-scaled H_2O covariance instead of using the measured $\delta^{18}O$ covariance. We determine the scaling factor (SF) which scales down the H_2O cospectral density to the $\delta^{18}O$ cospectral density by fitting the spectral powers to Eq. (6) for each 30 minute flux period. The only free variable is choosing a reasonable Low Pass Filter (LPF) that indicates until which frequency the spectra overlap reliably. We chose a LPF of 0.012 Hz based on visual inspection of various co spectra. We note that the resulting SF is hardly sensitive to the exact value of the LPF.

https://doi.org/10.5194/egusphere-2023-785
Preprint. Discussion started: 15 May 2023

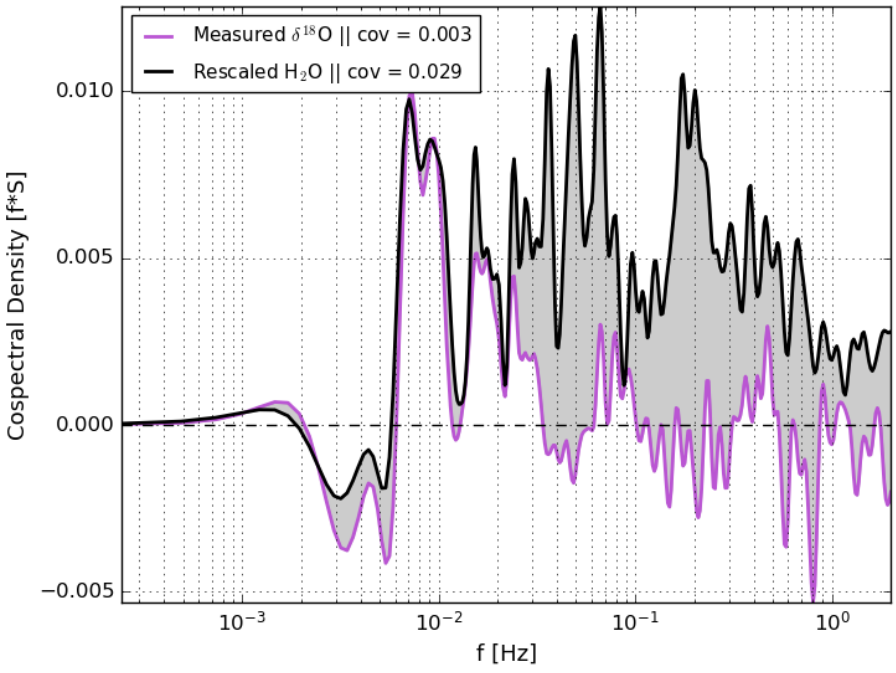

Figure 6. Cospectral analysis of δ^{18}O (of H_2O) and H_2O (from EC) with respect to w'. The H_2O spectrum was re-scaled to match the δ^{18}O spectrum at timescales longer then 100 seconds. The spectra are based on a 30 minute data interval taken during the measurement period starting at 14:00 on July 25^{th} 2021.

$$S_{\delta 18O}(f) = SF * S_{H2O}(f) + 0 \qquad where \qquad \begin{cases} f < LPF_{empirical} \\ and \\ sign(S_{\delta 18O}(f)) \equiv sign(S_{H2O}(f)) \end{cases} \tag{6}$$

Here, $S_{\delta^{18}O}(f)$ is the cospectral power of the raw δ^{18}O δ-flux, SF is the scaling factor, and $\text{LPF}_{empirical}$ is the empirically derived Low Pass Filter below which the two co spectra still overlap (see Fig. 6). Note that the equations above can be applied to any δ-flux but that the condition of the signs being equal is not universal. For example, during photosynthesis the CO_2 flux and δ^{13}C δ-flux are of opposite signs. The condition should thus be adjusted from $\equiv$ to $\neq$. Now, $S^*_{\delta 18O}(f)$ and $\overline{w'\delta^{18}O'^*}$, where $*$ denotes the corrected variable, can be defined as follows.

$$\overline{w'\delta^{18}O'^*} = \int S^*_{\delta 18O}(f)\, df = SF \int S_{H2O}(f)\, df = SF\overline{w'q'_x} \tag{7}$$

Additionally, we define the correction factors based on this spectral scaling technique.

https://doi.org/10.5194/egusphere-2023-785
Preprint. Discussion started: 15 May 2023

$$CF_{spec}^{\delta 18O} = \frac{\overline{w'\delta 18O'^{*}}}{\overline{w'\delta 18O'}} \quad (8)$$

The benefit of this δ-flux correction is that it is physically sound whether the cause of the missing high frequency signal is lacking sample throughput or isotopic exchange in the inlet line. Also, the δ-fluxes, which are essential for net ecosystem flux partitioning, do not need need to be calculated indirectly from corrected isotopologue fluxes, but are themselves the target variable. For our data set, we found that the δ-fluxes of H_2O were poorly resolved and that in most cases $CF_{spec}^{\delta 18O}$ & $CF_{spec}^{\delta D}$ » CF_{opga}^{H2O}. At the same time, the δ-fluxes of CO_2 were well resolved and $CF_{opga}^{CO2} \approx CF_{spec}^{\delta 13C} \approx CF_{spec}^{\delta 18O} \approx 1$ (see Sect. 5.2 and 5.3). The importance of this discrepancy between the H_2O and CO_2 signals and between CF_{spec} and CF_{opga}^{H2O} is discussed in Sect. 6.

5 Results

5.1 Time lag in isotopic signal

In addition to using the time alignment strategy described in Sect. 4.2, to synchronize the laser spectrometers with the Eddy Covariance system, we investigated the lag time of isotopic signals with respect to the mole fractions of the molecules. In theory, eddies with isotopically modified H_2O or CO_2 are expected to have deviations in mole fractions and δ-values that are proportional. When measuring such air parcels with the same instrument, at the same time, the δ-values and mole fractions should co-vary perfectly. Still, we found a time lag between H_2O and its isotopic signals of tens of seconds that had a strong diurnal cycle. Fig. 7 shows the pattern of the time lag between δD and H_2O over the measurement period. During night time, time lags were largest and often not resolved as no valid time lag could be identified. Note that the H_2O signal displayed was measured by the laser spectrometer and not by the OPGA.

In Fig. 7, the green dots are those time shifts which fall into the empirically derived range of time shifts, have sufficiently high correlation coefficients ($R^2 > 0.25$), and are part of a sequence of successive points which all comply with the first two rules. Consequently, the green dashed line connecting the green dots indicates the likely pattern in the time lag between the isotopic composition and the H_2O mole fraction. There are significant differences when inter-comparing days, but in the late afternoon - when temperatures are highest - the time lag is generally smallest. Red dots indicate that the time shifts had low R^2 values or that the time shifts deviated too strongly from its neighbours. We see clusters of red dots on the mornings of the 26^{th}, 27^{th} and 30^{th}, likely due to replacement of the inlet filter. In the discussion (Sect. 6), we will clarify why and how the time lag is related to this inlet filter.

The CO_2 signal and its δ-values do not suffer from a time offset in their signals. For $\delta^{13}C$, the lag time is 0 for the entire data-set, with few outliers. $\delta^{18}O$ has slightly more outliers. Additionally, we found a small time lag of approximately 2 seconds during midday that reoccurred diurnally (Appendix A2).

Evidently, the lag times we find are problematic for δ-flux calculations as they create an offset between w' and δ' (Eq. 2). To prevent this, we shifted the δ signals in time to match H_2O like explained in Sect. 4.2. On top of this, we discarded nighttime

https://doi.org/10.5194/egusphere-2023-785
Preprint. Discussion started: 15 May 2023

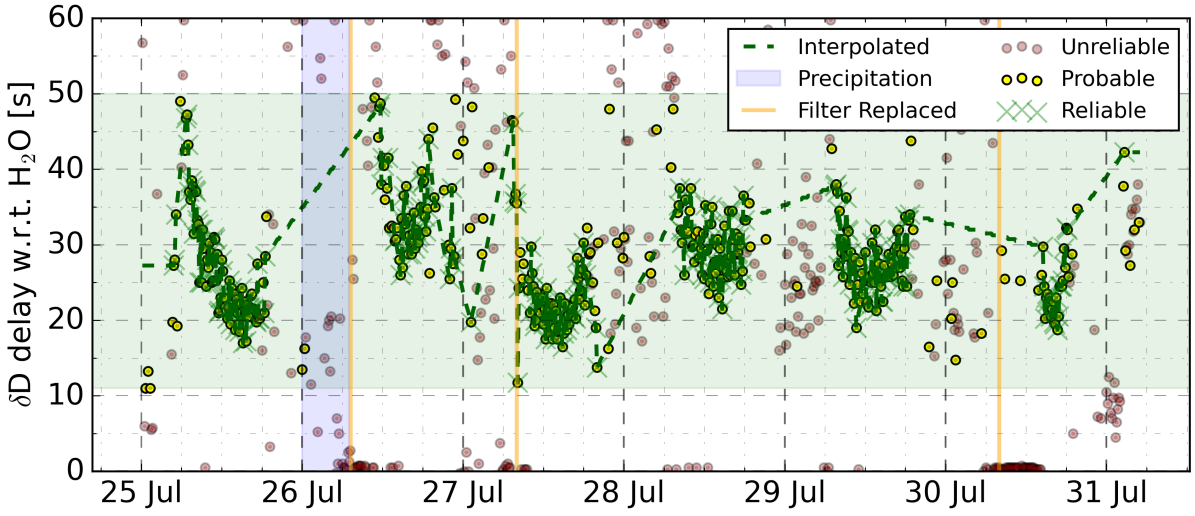

Figure 7. Time shifts between the δD and H_2O signals of the L2130-i analyzer. All symbols represent a 10 minute interval for which a time shift was derived. The red symbols indicate those intervals where the time shift was based on a low correlation coefficient ($R^2 < 0.25$) and or unlikely magnitude. The yellow symbols indicate that the time shift has a magnitude fitting within the general pattern of time lags (empirically set light green window) and an $R^2 > 0.25$ (See Fig. 4). The green symbols indicate the data-points which are part of a sequence of reliable "yellow" points. The dashed green line fitted through the green symbols was used to align the δ and H_2O signals.

data as no reliable time shift could be found. Note that the spectral corrections explained in Sect. 4.3.2 were applied after these time adjustments were made.

5.2 CO_2 Fluxes and isotopic signals

Using the time shift and spectral corrections, we generated a final output data set containing the various net ecosystem and δ-fluxes. Fig. 8 shows the CO_2 exchange fluxes between the fast growing alfalfa crop and the atmosphere.

Clear diurnal trends are visible in the CO_2 uptake and the δ^{13}C exchange flux. The sign of the net ecosystem exchange of CO_2 is as expected, demonstrating the dominance of photosynthesis during daytime and respiration at night. The total CO_2 flux signal derived from the closed cell CO_2 laser spectrometer matches the OPGA well. Similarly, the raw δ^{13}C and δ^{18}O δ-fluxes are comparable to the spectrally corrected variants. This gives confidence in our ability to resolve the δ-fluxes for CO_2 without needing to rely on corrections (Sect. 4.3.2). Note that the instability of the CO_2 analyser on longer timescales, as mentioned in Sect. 4.1, causes increased scatter in the spectrally scaled δ-flux signals compared to the raw δ-flux signals. The signs of the δ-flux indicates that during daytime photosynthetic uptake there is an upward transport of air parcels with higher δ^{13}C. This is in line with the fact that plants preferentially take up ^{12}C-CO_2, and follows the conceptual logic presented in Fig. 1. Panel D and E show the difference between the isotopic signature of the vertical flux and the ambient reservoir ($\Delta\delta^h X = \delta^h X_F - \delta^h X_{atm}$). For δ^{13}C, we observe that the surface reservoir is ≈ -15 ‰ more depleted in ^{13}C-CO_2 than the

https://doi.org/10.5194/egusphere-2023-785
Preprint. Discussion started: 15 May 2023

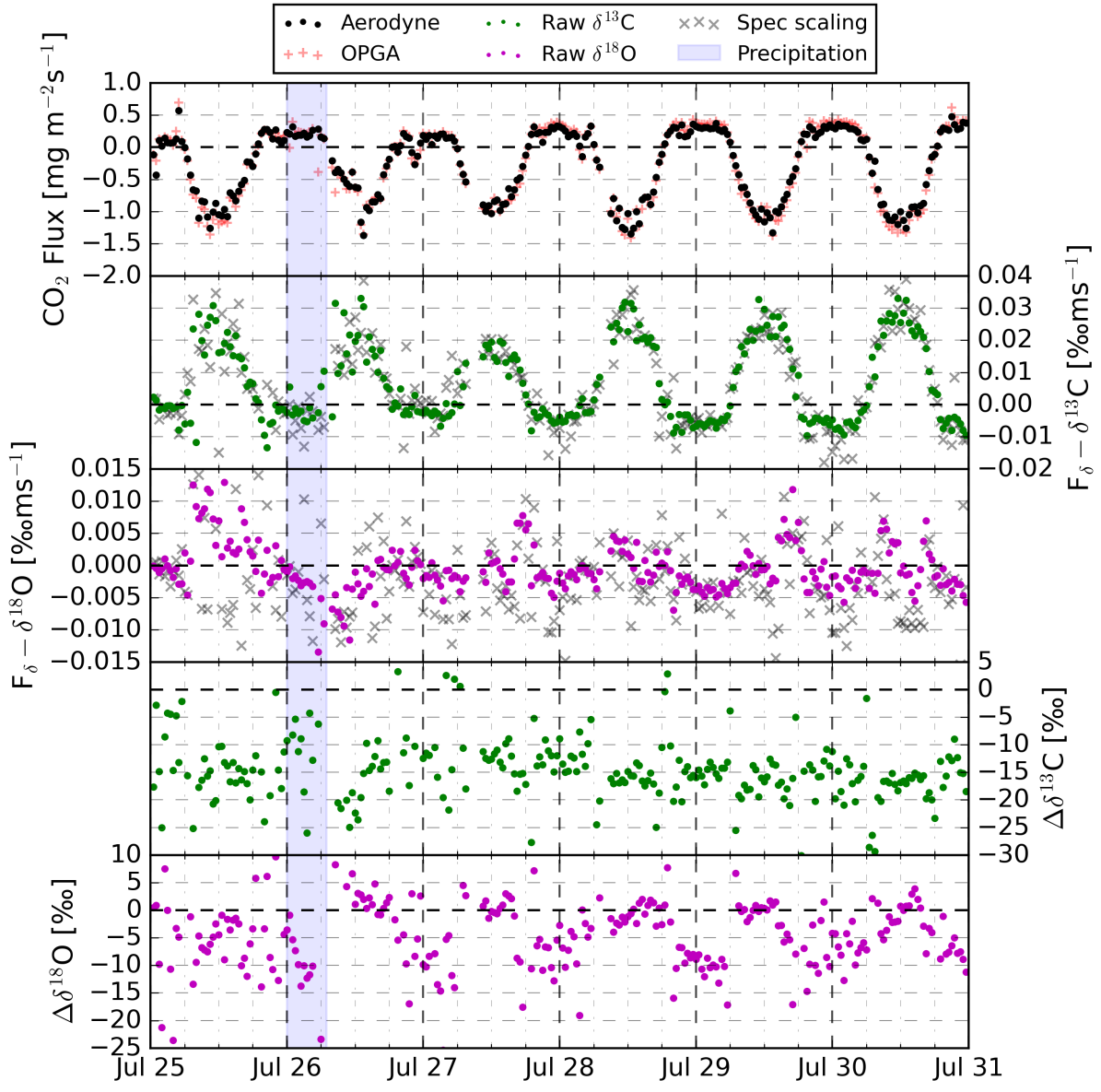

Figure 8. 30 minute CO_2 exchange fluxes over the 6 day measurement period above an alfalfa crop field near Mollerussa, Spain. Panel B and C display the δ-flux derived using Eq. (2). Panel D and E the difference in isotopic composition between the vertical exchange flux and atmosphere ($\delta^h X_F$ - $\delta^h X_{atm}$). The difference is plotted instead of both variables separately to eliminate the effect of instrument drift (see Sect. 4.1 on calibrations).

atmosphere. Given an atmospheric value of ≈-8‰, the vertical flux (or source) signature is -23‰, which is a typical value for the isotopic composition of C3 plants (Kohn, 2010).

https://doi.org/10.5194/egusphere-2023-785
Preprint. Discussion started: 15 May 2023

^{18}O δ-fluxes vary around zero, indicating small and variable atmospheric gradients caused by small differences between atmospheric and source compositions. In line with that, our daytime measurements show no notable difference between the isotopic composition of the vertical flux and the atmosphere ($\Delta\delta^{18}$O $\approx$ = 0, Fig. 8). This is not in line with the normative enrichment in the δ^{18}O-CO_2 signature near the earths surface over vegetated areas described in literature (Clog et al., 2015). Key processes impacting the δ^{18}O of CO_2 are generally the oxygen isotopic exchange in soil and leaf water, and diffusive fractionation of ^{18}O-CO_2 during plant assimilation (Rothfuss et al., 2013; Adnew et al., 2023). Given the large stomatal conductance (g_s) of the alfalfa crop in the footprint, diffusive fractionation effects will have been small (Adnew et al., 2020).

We pose that the water fed to the vegetation - and thus the soil - being largely melt water from the Pyrenees is the major cause of the small $\Delta\delta^{18}$O. This water will be more depleted compared to rain water because of the increased altitude at which droplets formed, and will thus lead to relatively ^{18}O-CO_2 depleted δ-fluxes during daytime (Gat et al., 2001; Yakir et al., 2006). Moreover, frequent irrigation events prevent strong enrichment of the liquid water in the top soil. Therefore, soil contributions to the respiration, and thus the $\delta^{18}O_F$, which get equilibrated with soil water under influence of Carbonic Anhydrase, will be more similar to $\delta^{18}O_{atm}$. The invasion of atmospheric CO_2 into and out of the soil, where oxygen isotopic equibrilation takes place, will contribute in a similar way (Wingate et al., 2009). Finally, oxygen exchange of CO_2 with H_2O in the plants mesophyll, where the water isotopic composition is linked to root-zone water from the Pyrenees, equally supports relatively depleted $\delta^{18}O_F$ (Yakir et al., 2006).

Another interesting feature visible in Fig. 8 is the effect of the precipitation event on δ^{18}O. The δ-fluxes become amplified and the source-atmosphere difference increases, most notably just after the precipitation event. It is not clear whether the δ^{18}O equibrilation of CO_2 with H_2O, responsible for changing F_δ-δ^{18}O (CO_2), predominantly takes place in the atmosphere, the soil, or in the mesophyll of plants.

5.3 H_2O fluxes and isotopic signals

In the previous section we indicated that the CO_2 isotope fluxes we measured were well resolved and therefore did not require corrections. This was not true for our H_2O isotope fluxes as large time shifts were required to realign the data set, and corrections for the signal loss at high frequency needed to be applied.

Fig. 9 shows an overview of the net ecosystem and isotopic exchange of water vapour over the 6 day measurement period. Clear diurnal patterns are visible in all variables, including the isotopic compositions of the flux displayed in panels D and E. The precipitation event on the 26^{th} reduces the magnitude of the Latent Heat Flux (L_vE) and deformes its diurnal pattern, likely due to cloud shading. The L_vE signal also reveals large differences between the gas exchange measured by the closed path instrument and the OPGA. In Sect. 4.3.1 we have shown that this is largely caused by missed high frequency variations in the H_2O signal. This ratio between the OPGA and the closed path instrument is not constant and is largest on the 25^{th} and the 30^{th}, and is equal to the magnitude of the OPGA scaling applied in panels B and C to the F_δ of δD and δ^{18}O. While the OPGA correction is significant, panel B and C reveal that the magnitude of the spectral scaling correction on the δ-fluxes is even larger (Sect. 6) which is in line with the loss of high frequency contributions to the δ-flux in Fig. 6.

https://doi.org/10.5194/egusphere-2023-785
Preprint. Discussion started: 15 May 2023

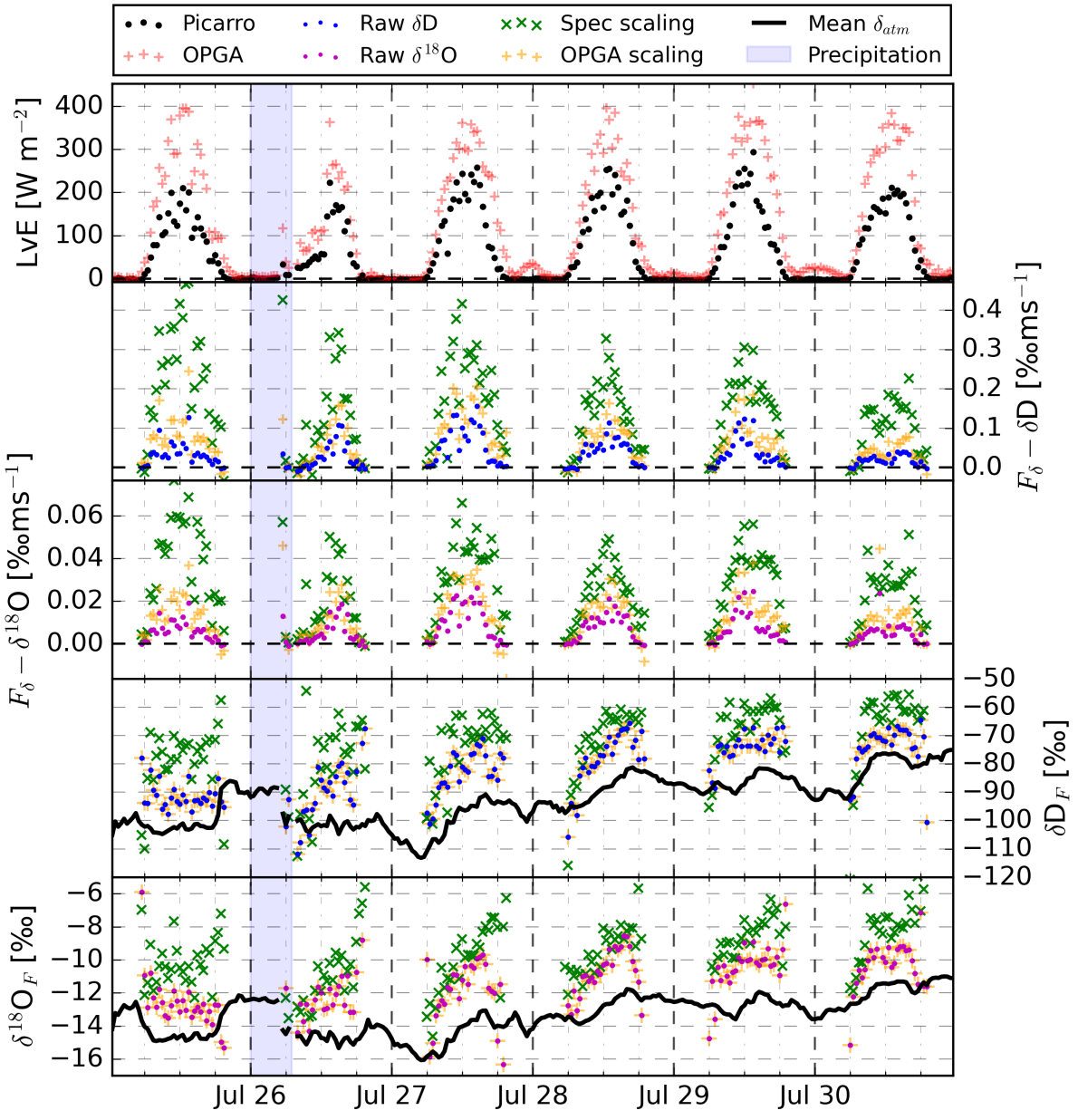

Figure 9. 30 minute H_2O exchange fluxes over the 6 day measurement period in Spain near Mollerussa. Panel B and C display the δ-flux derived using Eq. (2). Panel C and D indicate the isotopic composition of the vertical flux ($\delta^h X_F$) and the atmospheric background ($\delta^h X_{atm}$, black line). Panels B through E all contain three different symbols. The full circles represent the raw δ-fluxes or $\delta^h X_F$, while the yellow and green crosses indicate the corrected ones. These corrections are based on OPGA scaling like is common in isotope flux research (yellow), or on the Spectral scaling technique we detail in Sect. 4.3.2 (green).

https://doi.org/10.5194/egusphere-2023-785
Preprint. Discussion started: 15 May 2023

In terms of processes, transpiration dominated, and the δ-values in the stomata increase strongly during daytime due to the evaporative fractionation related to the transpiration. As a consequence, transpired water vapour is enriched in D and ^{18}O compared to the atmospheric background, which leads to isotope enrichment of air near the surface and ultimately to a negative vertical gradient (Fig. 1). In turn, the δ-fluxes are positive, transporting enriched water vapour up into the mixed layer. In line with that, the isotopic composition of the vertical flux ($\delta^h X_F$) starts at near atmospheric values in the early morning, and becomes enriched in the course of the day when transpiration persists and intensifies. This process and its effects on the isotopic signals is similar for δD and δ^{18}O.

6 Discussion

We have shown in our analysis that isotope flux measurements add information to state of the art H_2O or CO_2 net ecosystem exchanges flux measurements and atmospheric isotopic composition measurements. Still, obstacles like unreliable measurements and expensive instrumentation limit further implementation of the technique. Also, the scarce and possibly biased δ-flux data prevent further development of the partitioning method. To allow for more widespread implementation, corrections that ensure reliable δ-flux data are key. As mentioned above, δ-fluxes themselves are generally corrected using the signal loss in the net flux measured by the closed path laser spectrometer compared to the signal loss of the same net flux measured using an open path gas analyser (Wahl et al.; Oikawa et al., 2017; Wehr et al., 2013). We presented a different correction method based on spectral scaling, which suggests qualitatively different corrections. What are its consequences?

First, recall that in our H_2O laser spectrometer, mole fraction signals arrived before isotopologue signals with a time offset of tens of seconds that varied over the day. We know, for example from simple lab tests like breathing highly humid air into the inlet tube, that such time-offsets can be caused by condensation in the inlet. This is most probably caused by heavy isotopologues being more strongly bound to the liquid phase, and thus having a longer residence time in condensation droplets compared to light isotopologues. We expected that our preventive measures of using an actively heated inlet and high enclosure temperatures would have eliminated such condensation effects. However, in our setup during LIAISE the cellulose inlet filter was not heated. Likely, the hydrophilic nature of the material allowed for a small liquid water reservoir to form, which caused the isotopic exchange and consequent lag times that we observed in our data (Reishofer et al., 2022). In our data analysis we also made phase spectra to investigate if the time lag of the δ-values differed over the eddy sizes (similar to Peltola et al. (2021)). While we did not explore this in depth, it revealed clear differences in the time lag for larger and smaller eddy scales.

Despite these complications, we are confident in the reliability and accuracy of our measurements for the following reasons. First, we observe well defined cospectra for $\overline{w'q'}$ using the mole fractions measured by the H_2O laser spectrometer, which are to a great degree similar to those made with OPGA data. Secondly, after correcting for the lag times, we find δ-fluxes with cospectral signal, mainly at the lower frequencies. Finally, the δ-fluxes we resolve are of the sign we expect and follow logical diurnal cycles. Likely, the dampened isotopic signals have the same cause as the mole fraction - δ-value lag times: Isotopic exchange in the inlet. Missing cospectral signal in δ-fluxes and mole fraction fluxes is the rule rather than the exception in iso-flux measurements (Oikawa et al., 2017; Wahl et al.; Wehr et al., 2013). A possible cause of missing high frequency signal

https://doi.org/10.5194/egusphere-2023-785
Preprint. Discussion started: 15 May 2023

is lacking time resolution in the measurements. This can even occur when using the appropriate high frequency sensors when the re-flushing of the sample cell with new sample air takes longer then the analysis of a sample. However, we show that besides lacking sample separation due to limited flow rates or sampling frequency, isotopic exchange in the inlet line can also be a cause. We suggest using the lag time between mole fractions and δ-values as a diagnostic tool to identify inlet exchange, at least for H_2O. If such exchange is found to be present, spectra will certainly be affected and should be corrected appropriately.

We presented two options for correcting the spectra of isotopologue fluxes that differ significantly in their outcome. The OPGA based scaling method has been applied in previous studies and uses the lack in magnitude of the net exchange flux measured by an isotopologue analyser compared to an OPGA, to derive a correction factor with which all individual isotopologue fluxes are corrected. According to Eq. (3 & 4) this implies that the loss in δ-flux is as large as the loss in net exchange flux. We show that in cases where there is inlet exchange and attenuation, nonuniform time offsets between the isotopologues causes a greater loss covariance with w' for δ-values compared to the mole fractions of a molecule. These nonuniform time offsets will naturally affect eddies of shorter timescales more strongly. Therefore, our spectral scaling correction method only uses the signal from the very biggest and "longest" eddies. Conceptually, the covariance between two signals that are time offset by 10 seconds is not affected much at timescales > 100 seconds. One implication is that even if the goal is to measure mass fluxes of individual isotopologues, it is better to correct the δ-flux spectrum and use Eq. (3 & 4) to retrieve the corrected isotopologue concentrations.

Zooming in on the spectral scaling principle there is one fundamental assumption that requires further discussion. Namely, the assumption that eddies with altered concentrations of a mole fraction as a consequence of land atmosphere exchange have proportionally altered δ-values dependent on the process of exchange. In other words, the exchange cospectra of $\overline{w'CO_2'}$ and e.g. $\overline{w'\delta^{13}C'}$ should have identical shapes, irrespective of the sign. For the footprint of an EC station above a low crop, small eddies arising from specific leaves or soil sections will have undergone exchange and will now contain modified concentrations of CO_2 and H_2O. The added or removed molecules leave their specific isotopic fingerprints. Turbulence will organize eddies and mix this source signal into the Kolmogorov cascade of eddy scales to be detected by the EC station (Kolmogorov, 1941). All eddies, big or small, will then pick up part of the source signal. Essentially, the mole fraction and isotope effects of the surface source or sink will stay coupled and will thus be observable in a similar way throughout the scales of eddies.

To prove this hypothesis we can investigate the cospectra of δ-fluxes and mole fraction fluxes measured with a setup in which all turbulent scales are well represented. In Appendix A3 we show that the cospectral density for the $\delta^{13}C$ and CO_2 observations is generally very similar, supporting the validity of our hypothesis. While principle seems to hold, the $\delta^{13}C$ signal in Appendix A3 is impacted by instrument drift on long timescales and a relatively low signal to noise ratio. More precise experimental measurements of the net ecosystem exchange and net isotopic exchange of trace gasses affected by various fractionation processes should increase confidence in this hypothesis.

The spectral scaling technique that arises generates correction factors for the δ fluxes which deviate, in our case strongly, from the correction factors for the net exchange flux. This is of major importance as it will lead to a different flux partitioning. In this study, we do not expand on the consequences for partitioning much as we do not have strong constraints on all auxiliary variables that are needed for partitioning. However, isotopic ecosystem flux partitioning is impacted by our findings.

https://doi.org/10.5194/egusphere-2023-785
Preprint. Discussion started: 15 May 2023

The implications of the spectral scaling principle are broader than using it to find adequate corrections. If the hypotheses are correct, high frequency isotope measurements may not be required for 30 min average iso-flux determinations as we can infer the high frequency iso-flux contributions from the OPGA scaling. If we do not need to resolve the smallest eddies, setups can be simplified significantly by reducing inlet flow, increasing inlet line length, and setting up the analyser further away from the EC station. Also, there will most likely be a loss in precision of the determined δ-flux due to increased fitting errors in the spectral scaling technique. However, this can potentially be compensated by increased measurement precision through instrument development instead of increased measurement frequency. It opens the door to use cheaper, low flow rate isotope analysers to measure δ-fluxes at more ecosystem flux measurement sites.

6.1 Outlook

While 30 minute iso-fluxes - possibly measured with slower sensors in the future - are an appropriate way of validating flux partitioning, there are other open questions in land-atmosphere exchange that require high frequency iso-flux measurements. For example; how do intermittent cloud patterns impact the partial fluxes of H_2O and CO_2 at the second to minute scale? We know from previous investigations that land-atmosphere exchange behaves strongly non-linearly in such situations (Vilà-Guerau de Arellano et al., 2020). For example, continuous half shade results in much different exchange rates than alternating full shade and clear skies. In future work we aim to get to the core of such non-linearity's by making high time-resolution iso-flux measurements using a combination of high frequency isotopologue measurements and laser scintillometry (Van Kesteren et al., 2013; Vilà-Guerau de Arellano et al., 2019). With properly constrained auxiliary variables such measurements may allow us to derive partitioned minute scale fluxes of H_2O and CO_2.

A first quantification of how isotope exchange behaves at short timescales is presented in Fig. 10 in the form of a quadrant analyses (Shaw et al. (1983)). Here, the co-varying perturbations constituting the fluxes are plotted. This allows for background patterns to be investigated, such as the contributions of specific types of eddies. The tool can help us to visualize what happens within 30 minute flux period. Fig. 10 gives an example of such a quadrant plot during midday on the 25^{th} during the LIAISE campaign.

The covariance ($\overline{w'CO_2'}$) of the detrended w' and CO_2' signals laid out in Fig. 10 is the main component of to the net CO_2 flux ($\rho\ \overline{w'CO_2'}$). Clearly visible is the dynamic nature of the eddies within the 30 minute flux interval. See for example the blue blob at 0.15 $\mathrm{m\,s^{-1}}$ and 5 $\mu\mathrm{mol\,mol^{-1}}$. It is relatively depleted in $\delta^{13}\mathrm{C}$ indicating that this air parcel has not been enriched in $\delta^{13}\mathrm{C}$ through photosynthetic $^{12}CO_2$ uptake. In line with this, the CO_2 concentration of the air parcel is higher than the average at the altitude of the EC station. The air parcel however is moving up vertically towards the mixed layer, which is opposed to the flux direction. Still, on average, we find a clear pattern of depleted eddies with high CO_2 concentrations being carried towards the plants, and enriched eddies with reduced CO_2 contents being transported into the mixed layer. Individual air parcels moving upwards with reduced concentrations of CO_2 should indeed generally be enriched in $\delta^{13}\mathrm{C}$. This signal is in line with the photosynthetic fractionation process we described before.

Apart from visualizing the quasi random land-atmosphere exchange, a useful feature of figures like Fig. 10 is that residual layer air entrainment signals can be recognized and separated from surface influences (Efstathiou et al., 2020). In our case, the

https://doi.org/10.5194/egusphere-2023-785
Preprint. Discussion started: 15 May 2023

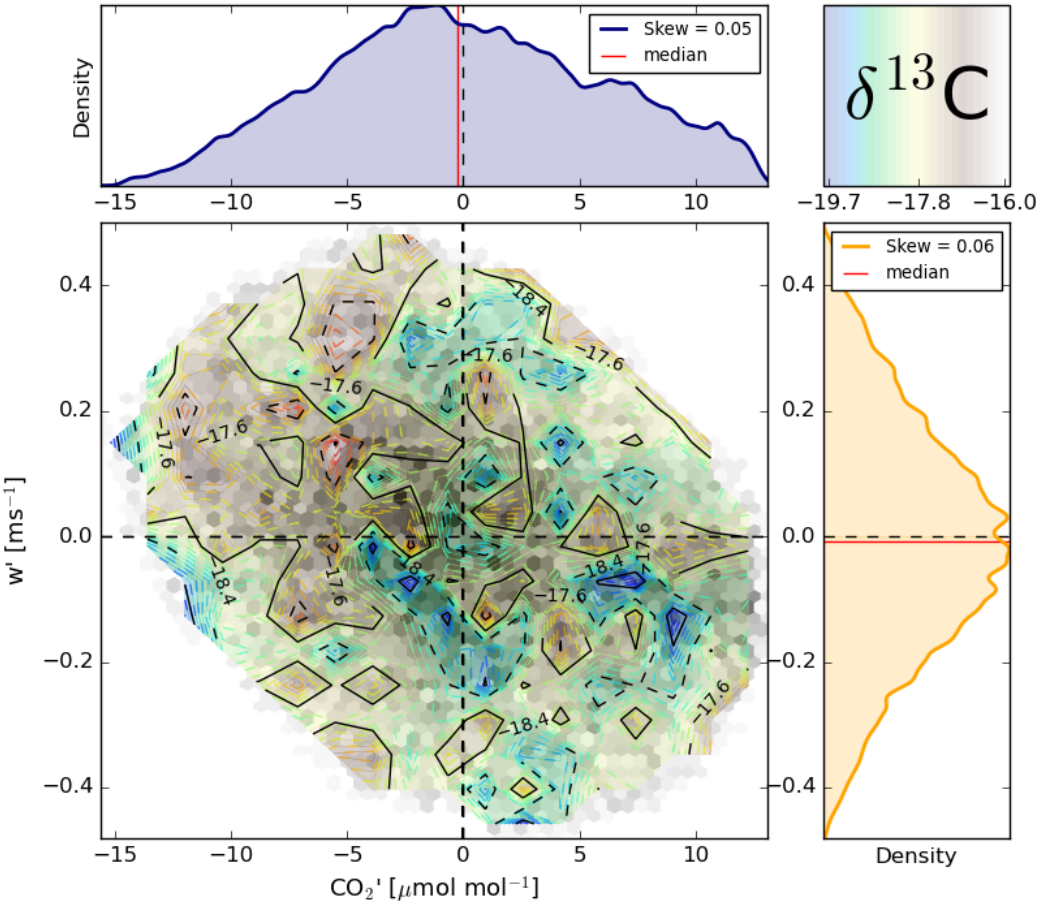

Figure 10. The land-atmosphere exchange of CO_2 within one 30 minute interval including the effect on δ^{13}C. The interval was taken from July 25^{th} at 14:30 UTC. The isotopic composition is indicated as a coloured contour plot over the w' and CO_2' parameter space which itself is plotted in black. Note that only the 90^{th} percentile contour of the quadrant figure is shown to allow for increased detail around the relevant dense center of the plot and prevent outliers in isotopic composition, CO_2 concentration and vertical wind speed to become dominant. Additionally, note that the absolute value of δ^{13}C is off.

bottom right quadrant shows some pockets of air with high CO_2 concentrations and low δ^{13}C values which must originate from higher up in the atmosphere. An intelligent algorithm could be designed to extract isotopic compositions of entraining air, which might be used as boundary conditions in model simulations (Lee et al., 2012; Vilà-Guerau de Arellano et al., 2019).

https://doi.org/10.5194/egusphere-2023-785
Preprint. Discussion started: 15 May 2023

7 Conclusions

We have presented methodological approach for measuring iso-fluxes during the LIAISE 2021 field campaign. The measurements encompass six days and are supported by comprehensive auxiliary data which pave the way for future modelling studies with integrated isotope effects. Our setup generally follows recommendations and procedures from previous studies but we introduced two key new concepts in terms of data processing. First, the idea of using the lag time between mole fractions and δ-values as a marker for isotopic inlet line attenuation. In our data, we find this to be important for the H_2O isotopologues we measured. We argue that when a time shift is detected, δ-flux spectra most probably lack more high frequency contributions compared to net exchange spectra. The second new concept is that of spectral scaling, which allows the asymmetric signal loss to be corrected for. This was required to correct the H_2O iso-fluxes that suffered from attenuation of the isotopic signal in the inlet line likely caused by a small liquid water reservoir. Finally, we illustrate the impact of this new spectral scaling technique on flux partitioning. Hopefully, the lessons we learned and tools we developed can be used to increase the precision, reliability, and shear number of measured iso-fluxes.

Author contributions. Robbert Moonen was responsible for the data aquisition, data processing, data analysis, and writing. Advanced technical support was provided by David Bonell Fontas, Getachew Adnew, and Oscar Hartogensis. Advanced scientific support was provided by Thomas Röckmann, Oscar Hartogensis, Jordi Vilà-Guerau de Arellano, and Getachew Adnew. All authors contributed to the finalization of the text.

Competing interests. The authors declare that they have no conflict of interest.

Acknowledgements. We would like to thank the NWO (OCENW.KLEIN.407) for providing funding for the CloudRoots Project (www.cloudroots.wur.nl). Also, we like to thanks the technical support and advice provided by Marcel Portanger, Paul Smeets, Henk Snelle, Roy Meinen, and Giorgio Cover. Finally, we would like to thank the staff of Aerodyne and Picarro for their support in working with their instruments.

https://doi.org/10.5194/egusphere-2023-785
Preprint. Discussion started: 15 May 2023

Appendix A

A1 Temporal evolution of δ^{13}C-CO_2 mole fraction calibrations

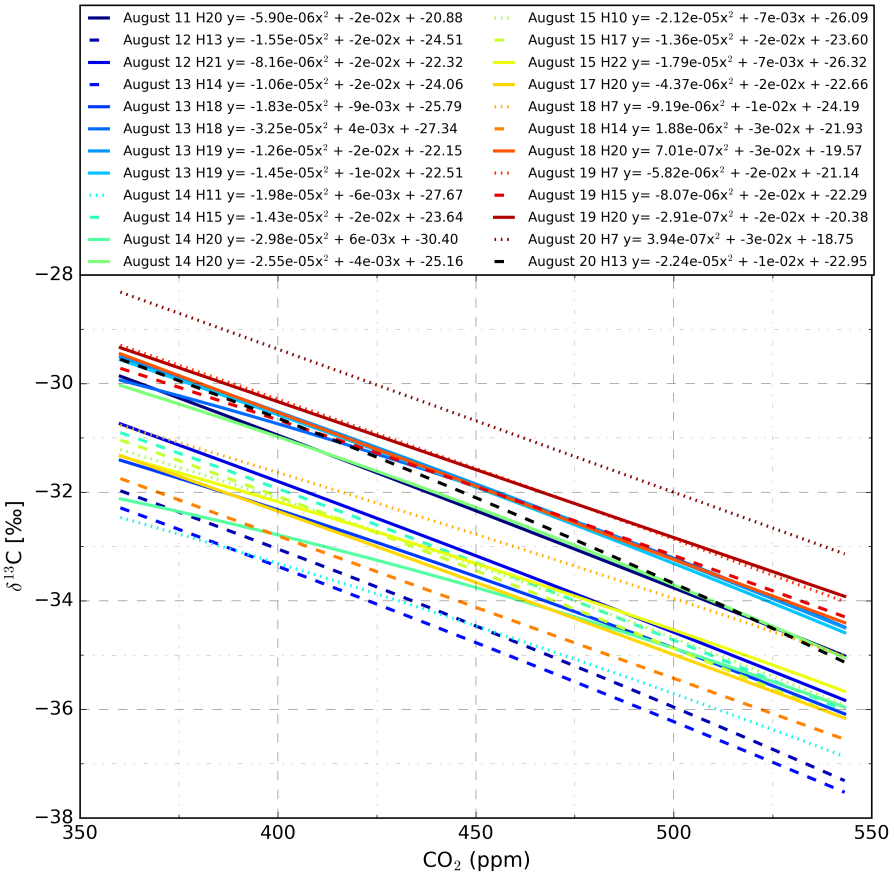

Figure A1. Mole fraction dependence of the Aerodyne TILDAS-CS instrument during operation at another measurement site. Similar to during the measurement period described in this document the isotopic composition measurements were was influenced by an artifact. Even though the absolute isotopic composition varied strongly over hourly timescales, mole fraction dependencies remained relatively constant during the 9 day period.

https://doi.org/10.5194/egusphere-2023-785
Preprint. Discussion started: 15 May 2023

A2 δ^{18}O-CO_2 time lag with respect to CO_2 mole fractions.

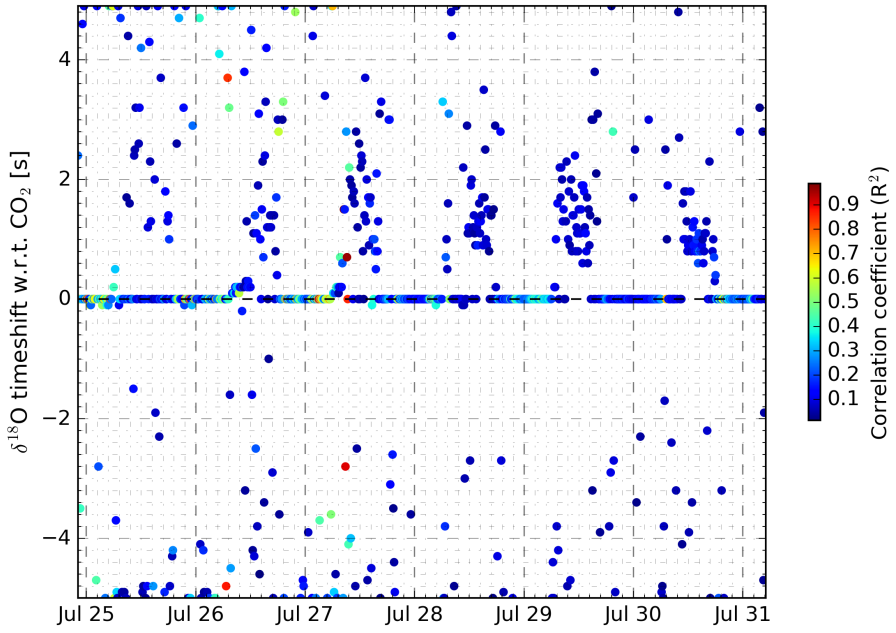

Figure A2. Time offset between CO_2 and its δ^{18}O isotope ratio derived using the method described in Sect. 4.2. The colors indicate the value of the correlation coefficient. Its value is generally low due to high frequency noise in the δ^{18}O signal.

https://doi.org/10.5194/egusphere-2023-785
Preprint. Discussion started: 15 May 2023

A3 Spectral scaling proof of concept using δ^{13}C-CO_2

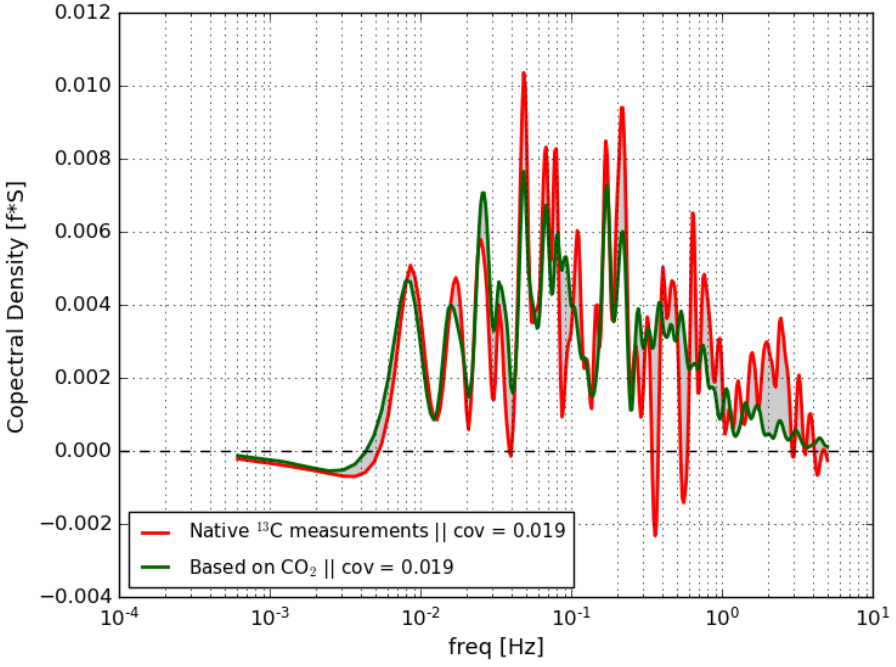

Figure A3. Example of the spectral scaling method applied to CO_2 isotopologue data which did not suffer from high frequency signal loss. The figure indicates that the spectral shapes of the δ-flux and the scaled down mole fraction flux are strongly related (Sect. 4.3.2). However, the increased noise in the lower signal to noise ratio causes the native δ^{13}C cospectrum to be more erratic.

https://doi.org/10.5194/egusphere-2023-785
Preprint. Discussion started: 15 May 2023

References

Adnew, G. A., Pons, T. L., Koren, G., Peters, W., and Röckmann, T.: Leaf-scale quantification of the effect of photosynthetic gas exchange on δ17O of atmospheric CO2, Biogeosciences, 17, 3903–3922, https://doi.org/10.5194/bg-17-3903-2020, 2020.

Adnew, G. A., Pons, T. L., Koren, G., Peters, W., and Röckmann, T.: Exploring the potential of Δ17O in CO2 for determining mesophyll conductance, Plant Physiology, https://doi.org/10.1093/plphys/kiad173/7082691, 2023.

Boone, A., Bellvert, J., Best, M., Brooke, J., Canut-Rocafort, G., Cuxart, J., Hartogensis, O., Le Moigne, P., Miró, R., and Polcher, J.: Updates on the International Land Surface Interactions with the Atmosphere over the Iberian Semi-Arid Environment (LIAISE) Field Campaign, Tech. rep., https://cw3e.ucsd.edu, 2021.

Clog, M., Stolper, D., and Eiler, J. M.: Kinetics of CO2(g)-H2O(1) isotopic exchange, including mass 47 isotopologues, Chemical Geology, 395, 1–10, https://doi.org/10.1016/j.chemgeo.2014.11.023, 2015.

Craig, H.: Isotopic standards for carbon and oxygen and correction factors for mass-spectrometric analysis of carbon dioxide, Geochimica et Cosmochimica Acta, 12, 133–149, https://doi.org/10.1016/0016-7037(57)90024-8, 1957.

Efstathiou, G. A., Thuburn, J., and Beare, R. J.: Diagnosing Coherent Structures in the Convective Boundary Layer by Optimizing Their Vertical Turbulent Scalar Transfer, Boundary-Layer Meteorology, 174, 119–144, https://doi.org/10.1007/s10546-019-00480-1, 2020.

Fan, S.-M., Wofsy, S. C., Bakwin, P. S., Jacob, D. J., and Fitzjarrald, D. R.: Atmosphere-biosphere exchange of CO2 and O3 in the central Amazon forest, Journal of Geophysical Research, 95, https://doi.org/10.1029/jd095id10p16851, 1990.

Farquhar, G. D., Erleringer, J. R., and Hubick, K. T.: Carbon Isotope Discrimination and Photosynthesis, Plant Physiology, 40, 503–537, 1989.

Gat, J. R., Mook, W. G., and Meijer, H. A. J.: Environmental isotopes in the hydrological cycle, Tech. rep., 2001.

Griffis, T. J.: Tracing the flow of carbon dioxide and water vapor between the biosphere and atmosphere: A review of optical isotope techniques and their application, Agricultural and Forest Meteorology, 174-175, 85–109, https://doi.org/10.1016/j.agrformet.2013.02.009, 2013.

Griffis, T. J., Baker, J. M., Sargent, S. D., Tanner, B. D., and Zhang, J.: Measuring field-scale isotopic CO2 fluxes with tunable diode laser absorption spectroscopy and micrometeorological techniques, Agricultural and Forest Meteorology, 124, 15–29, https://doi.org/10.1016/j.agrformet.2004.01.009, 2004.

Griffis, T. J., Zhang, J., Baker, J. M., Kljun, N., and Billmark, K.: Determining carbon isotope signatures from micrometeorological measurements: Implications for studying biosphere-atmosphere exchange processes, Boundary-Layer Meteorology, 123, 295–316, https://doi.org/10.1007/s10546-006-9143-8, 2007.

Griffis, T. J., Sargent, S. D., Lee, X., Baker, J. M., Greene, J., Erickson, M., Zhang, X., Billmark, K., Schultz, N., Xiao, W., and Hu, N.: Determining the Oxygen Isotope Composition of Evapotranspiration Using Eddy Covariance, Boundary-Layer Meteorology, 137, 307–326, https://doi.org/10.1007/s10546-010-9529-5, 2010.

Griffith, D. W. T.: Calibration of isotopologue-specific optical trace gas analysers: A practical guide, Atmospheric Measurement Techniques, https://doi.org/10.5194/amt-2018-187, 2018.

Horita, J. and Wesolowski, D. J.: Liquid-vapor fractionation of oxygen and hydrogen isotopes of water from the freezing to the critical temperature, Geochimica et Cosmochimica Acta, 58, 3425–3437, https://doi.org/10.1016/0016-7037(94)90096-5, 1994.

IAEA: Reference Sheet for International Measurement Standards VSMOW2, SLAP2, Tech. rep., IAEA, Vienna, 2017.

https://doi.org/10.5194/egusphere-2023-785
Preprint. Discussion started: 15 May 2023

Kohn, M. J.: Carbon isotope compositions of terrestrial C3 plants as indicators of (paleo)ecology and (paleo)climate, 107, https://doi.org/10.1073/pnas.1004933107/-/DCSupplemental, 2010.

Kolmogorov, A.: The local structure of turbulence in incompressible viscous fluid for very large Reynolds numbers, Cr. Acad. Sci. URSS, 30, 301–305, 1941.

Lee, X., Griffis, T. J., Baker, J. M., Billmark, K. A., Kim, K., and Welp, L. R.: Canopy-scale kinetic fractionation of atmospheric carbon dioxide and water vapor isotopes, Global Biogeochemical Cycles, 23, 1–15, https://doi.org/10.1029/2008GB003331, 2009.

Lee, X., Huang, J., and Patton, E. G.: A Large-Eddy Simulation Study of Water Vapour and Carbon Dioxide Isotopes in the Atmospheric Boundary Layer, Boundary-Layer Meteorology, 145, 229–248, https://doi.org/10.1007/s10546-011-9631-3, 2012.

Mangan, M. R., Hartogensis, O., Boone, A., Branch, O., Canut, G., Cuxart, J., de Boer, H. J., Le Page, M., Martínez-Villagrasa, D., Miró, J. R., Price, J., and Vilà-Guerau de Arellano, J.: The surface-boundary layer connection across spatial scales of irrigation-driven thermal heterogeneity: An integrated data and modeling study of the LIAISE field campaign, Agricultural and Forest Meteorology, 335, 109 452, https://doi.org/10.1016/j.agrformet.2023.109452, 2023.

Moene, A. F. and Van Dam, J. C.: Transport in the atmosphere-vegetation-soil continuum, Cambridge University Press, 2014.

Mook, W. G. and Geyh, M.: Environmental isotopes in the hydrological cycle, vol. 39, http://www.unesco.org/ulis/cgi-bin/ulis.pl?catno=121542&set=0054BFA545_1_47&gp=1&lin=1&ll=1, 2000.

Oikawa, P. Y., Sturtevant, C., Knox, S. H., Verfaillie, J., Huang, Y. W., and Baldocchi, D. D.: Revisiting the partitioning of net ecosystem exchange of CO2 into photosynthesis and respiration with simultaneous flux measurements of 13CO2 and CO2, soil respiration and a biophysical model, CANVEG, Agricultural and Forest Meteorology, 234-235, 149–163, https://doi.org/10.1016/j.agrformet.2016.12.016, 2017.

Peltola, O., Aslan, T., Ibrom, A., Nemitz, E., Rannik, U., and Mammarella, I.: The high-frequency response correction of eddy covariance fluxes - Part 1: An experimental approach and its interdependence with the time-lag estimation, Atmospheric Measurement Techniques, 14, 5071–5088, https://doi.org/10.5194/amt-14-5071-2021, 2021.

Picarro: Fastest, Most Precise Water Isotope Analysis Systems Accurately measure δ 18 O, δ 17 O, δD, and 17 O-excess in water quickly, simply, and without sample conversion, Tech. rep., Picarro INC., Santa Clara, 2021.

Prentice, I. C., Farquhar, G. D., Fasham, M. J. R., Goulden, M. L., Heimann, M., Jaramillo, V. J., Kheshgi, H. S., Le Quéré, C., Scholes, R. J., and Wallace, D. W. R.: The carbon cycle and atmospheric carbon dioxide, Tech. rep., https://hal.archives-ouvertes.fr/hal-03333974, 2001.

Reishofer, D., Resel, R., Sattelkow, J., Fischer, W. J., Niegelhell, K., Mohan, T., Kleinschek, K. S., Amenitsch, H., Plank, H., Tammelin, T., Kontturi, E., and Spirk, S.: Humidity Response of Cellulose Thin Films, Biomacromolecules, 23, 1148–1157, https://doi.org/10.1021/acs.biomac.1c01446, 2022.

Rothfuss, Y., Vereecken, H., and Brüggemann, N.: Towards a better understanding of the oxygen isotope signature of atmospheric CO2: Determining the 18O-exchange between CO2 and H2O in leaves and soil on-line with laser-based spectrometry, Tech. rep., Jülich, Forschungszentrum, Jülich, https://www.researchgate.net/publication/266398733, 2013.

Shaw, R. H., Tavangar, J., and Ward, D. P.: Structure of the Renolds Stress in a Canopy Layer, Journal of Climate and Applied Meteorology, 22, 1922–1931, 1983.

Spank, U. and Bernhofer, C.: Another simple method of spectral correction to obtain robust eddy-covariance results, Boundary-Layer Meteorology, 128, 403–422, https://doi.org/10.1007/s10546-008-9295-9, 2008.

https://doi.org/10.5194/egusphere-2023-785
Preprint. Discussion started: 15 May 2023

Sturm, P., Eugster, W., and Knohl, A.: Eddy covariance measurements of CO2 isotopologues with a quantum cascade laser absorption spectrometer, Agricultural and Forest Meteorology, 152, 73–82, https://doi.org/10.1016/j.agrformet.2011.09.007, 2012.

van Diepen, K. H. H., Goudriaan, J., Vilà-Guerau de Arellano, J., and de Boer, H. J.: Comparison of C3 Photosynthetic Responses to Light and CO 2 Predicted by the Leaf Photosynthesis Models of Farquhar et al. (1980) and Goudriaan et al. (1985), Journal of Advances in Modeling Earth Systems, 14, https://doi.org/10.1029/2021ms002976, 2022.

Van Kesteren, B., Hartogensis, O. K., van Dinther, D., Moene, A. F., De Bruin, H. A., and Holtslag, A. A.: Measuring H2O and CO2 fluxes at field scales with scintillometry: Part II - Validation and application of 1-min flux estimates, Agricultural and Forest Meteorology, 178-179, 88–105, https://doi.org/10.1016/j.agrformet.2013.01.010, 2013.

Vilà-Guerau de Arellano, J., Koren, G., Ouwersloot, H. G., van der Velde, I., Röckmann, T., and Miller, J. B.: Sub-diurnal variability of the carbon dioxide and water vapor isotopologues at the field observational scale, Agricultural and Forest Meteorology, 275, 114–135, https://doi.org/10.1016/j.agrformet.2019.05.014, 2019.

Vilà-Guerau de Arellano, J., Ney, P., Hartogensis, O., De Boer, H., Van Diepen, K., Emin, D., De Groot, G., Klosterhalfen, A., Langensiepen, M., Matveeva, M., Miranda-García, G., F. Moene, A., Rascher, U., Röckmann, T., Adnew, G., Brüggemann, N., Rothfuss, Y., and Graf, A.: CloudRoots: Integration of advanced instrumental techniques and process modelling of sub-hourly and sub-kilometre land-Atmosphere interactions, Biogeosciences, 17, 4375–4404, https://doi.org/10.5194/bg-17-4375-2020, 2020.

Vilà-Guerau de Arellano, J., Hartogensis, O., Benedict, I., de Boer, H., Bosman, P. J. M., Botía, S., Cecchini, M. A., Faassen, K. A. P., González-Armas, R., van Diepen, K., Heusinkveld, B. G., Janssens, M., Lobos-Roco, F., Luijkx, I. T., Machado, L. A. T., Mangan, M. R., Moene, A. F., Mol, W. B., van der Molen, M., Moonen, R., Ouwersloot, H. G., Park, S., Pedruzo-Bagazgoitia, X., Röckmann, T., Adnew, G. A., Ronda, R., Sikma, M., Schulte, R., van Stratum, B. J. H., Veerman, M. A., van Zanten, M. C., and van Heerwaarden, C. C.: Advancing understanding of land–atmosphere interactions by breaking discipline and scale barriers, Annals of the New York Academy of Sciences, https://doi.org/10.1111/nyas.14956, 2023.

Wahl, S., Steen-Larsen, H. C., and Reuder, J.: Quantifying the Stable Water Isotope Exchange between Snow Surface and Lower Atmosphere by Direct Flux Measurements.

Wehr, R. and Saleska, S. R.: An improved isotopic method for partitioning net ecosystem-atmosphere CO2 exchange, Agricultural and Forest Meteorology, 214-215, 515–531, https://doi.org/10.1016/j.agrformet.2015.09.009, 2015.

Wehr, R., Munger, J. W., Nelson, D. D., McManus, J. B., Zahniser, M. S., Wofsy, S. C., and Saleska, S. R.: Long-term eddy covariance measurements of the isotopic composition of the ecosystem-atmosphere exchange of CO2 in a temperate forest, Agricultural and Forest Meteorology, 181, 69–84, https://doi.org/10.1016/j.agrformet.2013.07.002, 2013.

Weng, Y., Touzeau, A., and Sodemann, H.: Correcting the impact of the isotope composition on the mixing ratio dependency of water vapour isotope measurements with cavity ring-down spectrometers, Atmospheric Measurement Techniques, 13, 3167–3190, https://doi.org/10.5194/amt-13-3167-2020, 2020.

Wingate, L., Ogée, J., Cuntz, M., Genty, B., Reiter, I., Seibt, U., Yakir, D., Maseyk, K., Pendall, E. G., Barbouri, M. M., Mortazavij, B., Burlett, R., Peylin, P., Miller, J., Mencuccini, M., Shim, J. H., Hunt, J., and Grace, J.: The impact of soil microorganisms on the global budget of δ18O in atmospheric CO2, Proceedings of the National Academy of Sciences of the United States of America, 106, 22 411–22 415, https://doi.org/10.1073/pnas.0905210106, 2009.

Yakir, D., Berry, J., Giles, L., and Osmond, C.: Isotopic heterogeneity of water in transpiring leaves: Identification of the component that controls the delta18O of atmospheric O2 and CO2, Plant, Cell & Environment, 17, 73 – 80, https://doi.org/10.1111/j.1365-3040.1994.tb00267.x, 2006.